

Molecular Cloning and Characterization of a Novel 3'-Phosphoadenosine 5'-Phosphosulfate Transporter, PAPST2*

Received for publication, August 15, 2005, and in revised form, February 8, 2006 Published, JBC Papers in Press, February 21, 2006, DOI 10.1074/jbc.M508991200

Shin Kamiyama^{‡§}, Norihiko Sasaki^{‡¶}, Emi Goda^{‡¶}, Kumiko Ui-Tei^{||}, Kaoru Saigo^{||}, Hisashi Narimatsu^{**}, Yoshifumi Jigami^{**}, Reiji Kannagi^{††}, Tatsuro Irimura^{§§}, and Shoko Nishihara^{‡¶1}

From the [‡]Laboratory of Cell Biology, Department of Bioinformatics, Soka University, 1-236 Tangi-cho, Hachioji, Tokyo 192-8577, [§]Research Association for Biotechnology, 3-9, Nishi-Shinbashi 2-chome, Minato-ku, Tokyo 105-0003, [¶]Core Research for Evolutional Science and Technology of Japan Science and Technology Agency, Kawaguchi Center Building, 4-1-8, Hon-cho, Kawaguchi, Saitama 332-0012, ^{||}Department of Biophysics and Biochemistry, Graduate School of Science, The University of Tokyo, 7-3-1 Hongo, Bunkyo-ku, Tokyo 113-0033, ^{**}Research Center for Glycoscience, National Institute of Advanced Industrial Science and Technology, 1-1-1 Umezono, Tsukuba, Ibaraki, 305-8586, ^{††}Program of Molecular Pathology, Aichi Cancer Center, 1-1 Kanokoden, Chikusa-ku, Nagoya 464-8681, and ^{§§}Laboratory of Cancer Biology and Molecular Immunology, Graduate School of Pharmaceutical Sciences, The University of Tokyo, 7-3-1 Hongo, Bunkyo-ku, Tokyo 113-0033, Japan

Sulfation is an important posttranslational modification associated with a variety of molecules. It requires the involvement of the high energy form of the universal sulfate donor, 3'-phosphoadenosine 5'-phosphosulfate (PAPS). Recently, we identified a PAPS transporter gene in both humans and *Drosophila*. Although human colonic epithelial tissues express many sulfated glycoconjugates, *PAPST1* expression in the colon is trace. In the present study, we identified a novel human PAPS transporter gene that is closely related to human *PAPST1*. This gene, called *PAPST2*, is predominantly expressed in human colon tissues. The *PAPST2* protein is localized on the Golgi apparatus in a manner similar to the *PAPST1* protein. By using yeast expression studies, *PAPST2* protein was shown to have PAPS transport activity with an apparent K_m value of 2.2 μM , which is comparable with that of *PAPST1* (0.8 μM). Overexpression of either the *PAPST1* or *PAPST2* gene increased PAPS transport activity in human colon cancer HCT116 cells. The RNA interference of the *PAPST2* gene in the HCT116 cells significantly reduced the reactivity of G72 antibody directed against the sialyl 6-sulfo *N*-acetylglucosamine epitope and total sulfate incorporation into cellular proteins. These findings indicate that *PAPST2* is a PAPS transporter gene involved in the synthesis of sulfated glycoconjugates in the colon.

Sulfation of a variety of molecules, including glycoproteins, proteoglycans, and glycolipids, is an important posttranslational modification. The process requires the involvement of the high energy form of the universal sulfate donor, namely, 3'-phosphoadenosine 5'-phosphosulfate (PAPS).² In higher organisms, PAPS is synthesized in the cytosol or nucleus by PAPS synthetases (1, 2) and is subsequently translocated into

the Golgi lumen via the PAPS transporter(s). Because most of the sulfation of glycoconjugates occurs in the Golgi apparatus, the translocation of PAPS is considered to be an essential process.

Recently, we identified and characterized a PAPS transporter in both humans and *Drosophila* (3). Human *PAPST1* and the *Drosophila* ortholog *SLALOM* (*SLL*) are Golgi-localized proteins that exhibit PAPS-specific transport activity. Analysis of the *sll* gene by using the RNA interference (RNAi) fly demonstrated that the PAPS transporter is essential for viability *in vivo* (3). Furthermore, Lüders *et al.* (4) demonstrated that *sll* is involved in growth factor signaling pathways during patterning and morphogenesis. Heparan sulfate proteoglycans (HSPGs) possess glycosaminoglycan chains that contain diversely sulfated uronic acid and glucosamine residues. Cell surface HSPGs are involved in a variety of developmental signaling pathways, and the functions of HSPGs are dependent on their sulfation state (5–10). A mutation in the *sll* gene caused defects in multiple signaling pathways, including Wingless and Hedgehog signaling, probably because of the lack of HSPG sulfation (4).

Despite the low expression of the *PAPST1* gene in the colon (3), human colonic tissues highly express many sulfated glycoconjugates such as proteoglycans and sulfomucins. For example, the 3'-sulfo Lewis a epitope (3'-sulfo Le^a: Gal β 1,3 (fucose α 1,4) GlcNAc that is sulfated at the C-3 position of Gal) is strongly expressed in the normal colonic epithelium but diminishes considerably in primary colon carcinomas (11–13). The sialyl 6-sulfo Lewis x epitope (sialyl 6-sulfo Le^x: Sia α 2,3 Gal β 1,4 (fucose α 1,3) GlcNAc that is sulfated at the C-6 position of GlcNAc) is also expressed in normal human colonic tissues but not in cancerous tissues (14). These sulfated glycoconjugate epitopes are believed to regulate many biological processes in the colon (11–17).

In the present study, we attempted to identify the PAPS transporter that is responsible for the sulfation of glycoconjugates in the colon tissue. We found a gene that is closely related to the human *PAPST1* gene by performing a BLAST search of data bases. This gene, called *PAPST2*, is preferentially expressed in human colon tissues. The *PAPST2* protein exhibited PAPS transport activity similar to that of the *PAPST1* protein. Here, we report the functional properties of this novel PAPS transporter.

* This work was supported by Core Research for Evolutional Science and Technology of the Japan Science and Technology Agency and the New Energy and Industrial Technology Development Organization. The costs of publication of this article were defrayed in part by the payment of page charges. This article must therefore be hereby marked "advertisement" in accordance with 18 U.S.C. Section 1734 solely to indicate this fact.

The nucleotide sequence(s) reported in this paper has been submitted to the DDBJ/GenBank™/EBI Data Bank with accession number(s) AB231931.

¹ To whom correspondence should be addressed. Tel./Fax: 81-426-91-8140; E-mail: shoko@t.soka.ac.jp.

² The abbreviations used are: PAPS, 3'-phosphoadenosine 5'-phosphosulfate; FITC, fluorescein isothiocyanate; Gal, galactose; GAPDH, glyceraldehyde-3-phosphate dehydrogenase; GlcNAc, UDP-*N*-acetyl D -glucosamine; HA, influenza hemagglutinin epitope; Le^a, Lewis x antigen, galactose β 1,4 (fucose α 1,3) *N*-acetyl D -glucosamine; Le^s, Lewis a antigen, galactose β 1,3 (fucose α 1,4) *N*-acetyl D -glucosamine; mAb,

monoclonal antibody; PBS, phosphate-buffered saline; RNAi, RNA interference; siRNA, small interfering RNA; *sll*, *slalom*.

EXPERIMENTAL PROCEDURES

Materials—GDP-[2-³H]mannose (15 Ci/mmol), UDP-[1-³H]glucose (15 Ci/mmol), UDP-*N*-acetyl [6-³H]D-galactosamine (15 Ci/mmol), UDP-[¹⁴C(U)]glucuronic acid (15 Ci/mmol), and carrier-free [³⁵S]H₂SO₄ (100 m Ci/ml) were purchased from American Radiolabeled Chemicals Inc. (St. Louis, MO). GDP-[1-³H]fucose (6.95 Ci/mmol), UDP-[4,5-³H]galactose (48.3 Ci/mmol), CMP-[9-³H]sialic acid (33.6 Ci/mmol), UDP-*N*-acetyl [6-³H(N)]D-glucosamine (39.7 Ci/mmol), and [³⁵S]PAPS (1.82 Ci/mmol) were purchased from Perkin Elmer Life Sciences Inc. Zymolyase 100T was obtained from Seikagaku Kogyo Co. Ltd. (Tokyo, Japan). Fluorescein isothiocyanate (FITC)-conjugated anti-c-Myc monoclonal antibody (mAb) (9E10) and rhodamine-conjugated anti-influenza hemagglutinin epitope (HA) mAb (HA-probe, F-7) were obtained from Santa Cruz Biotechnology, Inc. (Santa Cruz, CA). All the other reagents used in the study were of the highest purity grade available commercially.

Isolation of Human PAPS Transporter cDNA and Construction of Expression Plasmids—The human *PAPST2* gene was identified and cloned using the same procedures as described previously (3). The amino acid sequence of the open reading frame of *UGTrel1* (18) was used as a query sequence for the TBLASTN search that was performed to detect novel genes. To obtain the cDNA of NM_015948, a human gene that was identified in this study, and to create recombination sites for the GATEWAY™ cloning system (Invitrogen), we used two steps of *attB* adaptor PCR and prepared *attB*-flanked PCR products. For the first gene-specific amplification, a forward template-specific primer with *attB1*, 5'-AAAAAGCAGGCTTCCATAATGGCATGGACTTG-3', and a reverse template-specific primer with *attB2*, 5'-AGAAAGCTGGGTCTACAGTCTGTGCCAGCGT-3', were used. PCR was performed using Platinum® Pfx DNA polymerase (Invitrogen) and a cDNA library derived from human colon tissue. The insertion of a complete *attB* adaptor and cloning into the pDONR™201 vector were performed in accordance with the manufacturer's protocol to create an entry clone for use during the subsequent subcloning steps.

The entry clone was subcloned into the appropriate expression vectors by using the GATEWAY™ cloning system in accordance with the manufacturer's protocol. A 3 × HA epitope tag or a c-Myc tag was inserted into the expression vectors at the position corresponding to the C terminus of the expressing protein.

Transient Transfection and Immunofluorescence Microscopy—Transient transfection and immunofluorescence microscopy were performed by using one of two procedures. The first procedure is similar to one described previously (3, 19). Briefly, HCT116 cells were subcultured onto a 4-well Lab-Tek chamber slide (Nalge Nunc International) in Dulbecco's modified Eagle's medium/Ham's nutrient mixture F-12 (1:1) containing 10% fetal bovine serum. After 24 h of subculturing, the HCT116 cells were transfected with 0.25 μg/well of pCXN2 (20), pCXN2 inserted with HA-tagged *PAPST1*, or pCXN2 inserted with HA-tagged *PAPST2* by using Lipofectamine 2000 reagent (Invitrogen) in accordance with the manufacturer's protocol. After 72 h, the cells were fixed in phosphate-buffered saline (PBS) containing 4% paraformaldehyde for 30 min at 4 °C, and they were then permeabilized in a permeabilizing buffer (PBS containing 0.1% Triton X-100) for 1 h at 4 °C. The cells were subsequently double immunostained with rhodamine-conjugated anti-HA mAb and anti-β1,4-galactosyltransferase 1 mAb (21) as described previously (3, 19). Finally, the cells were washed four times and mounted with PermaFluor (Thermo Shandon, Pittsburgh, PA). The fluorescence was observed using a confocal laser scanning microscope, LSM5 Pascal (Carl Zeiss, Goettingen, Germany). In the second procedure, HA-tagged *PAPST2* and c-Myc-tagged *PAPST1*

were expressed simultaneously in the HCT116 cells. After 24 h of subculturing, the cells were transfected with 0.25 μg/well of pCXN2 or pCXN2 inserted with HA-tagged *PAPST2* and pCXN2 inserted with c-Myc-tagged *PAPST1* by using Lipofectamine 2000 reagent. The cells were fixed, permeabilized, and immunostained with FITC-conjugated anti-c-Myc mAb and rhodamine-conjugated anti-HA mAb for 30 min at 37 °C after 72 h. The remainder of the procedure was the same as that described above.

Stable Transfection and Subcellular Fractionation—HCT116 cells were subcultured onto 6-cm dishes in Dulbecco's modified Eagle's medium/Ham's nutrient mixture F-12 (1:1) containing 10% fetal bovine serum. After 24 h, the cells were transfected with 8 μg of pCXN2 vector, pCXN2 inserted with HA-tagged *PAPST1*, or pCXN2 inserted with HA-tagged *PAPST2* by using Lipofectamine 2000 reagent in accordance with the manufacturer's protocol. The transfectants were selected by the addition of 600 μg/ml of geneticin (Invitrogen) to the medium and cultured for 1 month after 48 h.

Subcellular fractionation was performed as described previously (3, 19). The cells were harvested and suspended in 10 mM HEPES-Tris (pH 7.4) containing 0.25 M sucrose, 1 mM phenylmethylsulfonyl fluoride, and 1 μg/ml each of leupeptin, aprotinin, and pepstatin A. The cells were then homogenized using a Dounce homogenizer. The lysate was centrifuged at 1,000 × *g* for 10 min to remove the unlysed cells and cell wall debris. The supernatant was then centrifuged at 7,700 × *g* for 10 min at 4 °C, and the supernatant was further centrifuged at 100,000 × *g* to yield a pellet of P100 membrane fraction.

Subcellular Fractionation of Yeast and Transport Assay—Yeast (*Saccharomyces cerevisiae*) strain W303-1a (*MATa*, *ade2-1*, *ura3-1*, *his3-11,15*, *trp1-1*, *leu2-3,112*, and *can1-100*) was transformed by the lithium acetate procedure (22) using a yeast expression vector, YEp352GAP-II (23). These transformed yeast cells were grown at 30 °C in a synthetic defined medium, which did not contain uracil, for selecting transformants. Subcellular fractionation and nucleotide sugar transport assays were performed as described previously (3, 19). The cells were harvested, washed with ice-cold 10 mM Na₂S₂O₃, and converted into spheroplasts by incubation at 37 °C for 30 min in spheroplast buffer (1.4 M sorbitol, 50 mM potassium phosphate (pH 7.5), 10 mM Na₂S₂O₃, 40 mM 2-mercaptoethanol, and 1 mg of Zymolyase 100T/g of cells). The spheroplasts were pelleted using a refrigerated centrifuge and washed twice with 1.0 M ice-cold sorbitol to remove traces of zymolyase. The cells were suspended in ice-cold lysis buffer (0.8 M sorbitol in 10 mM triethanolamine (pH 7.2), 5 μg/ml of pepstatin A, and 1 mM phenylmethylsulfonyl fluoride) and subsequently homogenized using a Dounce homogenizer. The lysate was centrifuged at 1,000 × *g* for 10 min to remove the unlysed cells and cell wall debris. The supernatant was then centrifuged at 10,000 × *g* for 15 min at 4 °C, which yielded a pellet of P10 membrane fraction. The supernatant was further centrifuged at 100,000 × *g* to yield a pellet of P100 membrane fraction. Each fraction (200 μg of protein) was then incubated in 100 μl of reaction buffer (20 mM Tris-HCl (pH 7.5), 0.25 M sucrose, 5.0 mM MgCl₂, 1.0 mM MnCl₂, and 10 mM 2-mercaptoethanol) that contained 1 μM radiolabeled substrate at 30 °C for 5 min. After incubation, the radioactivity incorporated in the microsomes was trapped using a 0.45-μm nitrocellulose filter and measured using liquid scintillation. The amount of incorporated radioactivity was calculated as the difference from the background value obtained from the same assay at 30 °C for 0 min for each sample.

Western Blot Analysis—Fifty micrograms of protein from each sample was added to 3× sodium dodecyl sulfate (SDS) sample buffer (New England Biolabs Inc., Beverly, MA) and subsequently incubated at room

temperature for 2 h. The samples were fractionated on a 2–15% SDS-polyacrylamide gel gradient (Daiichi Pure Chemicals Co., Ltd., Tokyo, Japan). The separated proteins were electrotransferred onto a polyvinylidene difluoride membrane. The HA-tagged proteins were immunostained with anti-HA mouse mAb and horseradish peroxidase-conjugated anti-mouse IgG mAb. Bound horseradish peroxidase was detected using ECL plus (Amersham Biosciences) in accordance with the manufacturer's instructions.

Quantitative Analysis of the PAPST2 Transcript in Human Tissues by Real-time PCR—The amount of *PAPST1* and *PAPST2* transcripts in human tissues was determined by real-time PCR. Total RNA was extracted from human tissues by the method of Chomczynski and Sacchi (24). First strand cDNA was synthesized using a Superscript II First Strand Synthesis kit (Invitrogen) in accordance with the manufacturer's instructions. Real-time PCR was performed using a qPCR Mastermix (QuickGoldStar; Eurogentec, Seraing, Belgium) and ABI PRISM 7700 Sequence Detection System (Applied Biosystems, Foster, CA). The PCR primer pair sequences and TaqMan probes used for each gene were as follows. For the detection of *PAPST1*, the forward primer 5'-GGCAGGCCCTGAAGCT-3', reverse primer 5'-TGCGGGTCATCACTCTTTC-3', and probe 5'-CCACAGGGCTCCAGGTGTCTTATCTG-3' were used. For the detection of *PAPST2*, the forward primer 5'-GATTAGGCCCTGCAGTAACATT-3', reverse primer 5'-ATCCAGTAGGGAAAAAGGA-3', and probe 5'-TGTGCAAAGAATCCAGTTCGGACCTA-3' were used. The probes were labeled at the 5'-end with the reporter dye FAM and at the 3'-end with the quencher dye TAMRA. The relative amounts of *PAPST1* and *PAPST2* transcripts were normalized with respect to the human glyceraldehyde 3-phosphate dehydrogenase (*GAPDH*) transcripts present in the same cDNA.

Northern Blot Analysis—*PAPST2* cDNA probe (full-length open reading frame) was prepared by random priming using [α - 32 P]dCTP and BcaBestTM labeling kit (Takara Bio Inc., Shiga, Japan) in accordance with the manufacturer's instructions. Poly(A)⁺ RNA was isolated using Oligotex-dT30 (super) mRNA purification kit (Takara Bio Inc.) in accordance with the manufacturer's instructions. Poly(A)⁺ RNA derived from each sample was separated by 1.2% agarose gel containing 2.2 M formaldehyde and then transferred onto Hybond-XL nylon membrane (Amersham Biosciences). The membranes were prehybridized in the hybridization solution (5× SSPE (standard saline phosphate with EDTA; 150 mM NaCl, 10 mM NaH₂PO₄, 1 mM EDTA), 5× Denhardt's solution, and 0.2 mg/ml of salmon sperm DNA) for 2 h at 42 °C. The membranes were hybridized overnight in hybridization solution containing 2 × 10⁶ cpm/ml of each radiolabeled probe at 42 °C. Following hybridization, the membrane was washed in 2× SSPE containing 0.1% SDS at room temperature and in 0.2× SSPE containing 0.1% SDS at 50 °C. The radiolabeled materials were detected by using a BAS-2000 imaging analyzer (Fuji Photo Film). The membrane was reprobed with a human *GAPDH* cDNA probe.

RNAi of PAPST2 Gene—A sequence of small interfering RNA (siRNA) for each gene was designed as described previously (25). Twenty-five base pairs of stealth RNAs were designed and purchased from Invitrogen. The PAPST1–813 siRNA (initiated at the 813 nucleotide position from the start codon) has the sequence 5'-CCUCAUCU-UACUGGCAGGUUAUUAU-3'. The sequences of PAPST2–342 siRNA (initiated at the 342 nucleotide position from the start codon) and PAPST2–513 siRNA (initiated at the 513 nucleotide position from the start codon) are 5'-CCUUAACCUUAGUGCAGUUUGCCUUU-3' and 5'-CCAAGUCAUCUUAAGUGCUGCAAAA-3', respectively. As control siRNA, stealth RNAi negative control duplex (Invitrogen) was used. The HCT116 cells were subcultured onto 6-cm dishes at a con-

centration of 1 × 10⁶ cells/dish in Dulbecco's modified Eagle's medium/Ham's nutrient mixture F-12 (1:1) containing 10% fetal bovine serum 24 h prior to the transfection. The cells were transfected with 10 or 100 nM siRNA by using Lipofectamine 2000 reagent. RNA was extracted using TRIzol reagent (Invitrogen), and the first strand cDNA was synthesized using a Superscript II First Strand Synthesis kit (Invitrogen).

Metabolic Labeling of Colon Cancer Cell Line—Radiolabeling of sulfated residues in cell macromolecules was performed using procedures similar to those described previously (26). HCT116 cells were subcultured onto 10-cm dishes at a concentration of 1.5 or 2 × 10⁶ cells/dish in the inorganic sulfate-free Dulbecco's modified Eagle's medium/Ham's nutrient mixture F-12 (1:1) containing 10% fetal bovine serum and 100 μ Ci/ml of carrier-free [35 S]H₂SO₄ 48 h after transfection and 48 h prior to the analysis. The cells were rinsed with PBS and detached with PBS containing 0.02% EDTA for 5 min. The cells were rinsed twice with PBS and suspended in 4 volumes of lysis buffer (10 mM Tris-HCl (pH 7.4), 0.5% Nonidet P-40, 1 mM EDTA, and 0.5 mM phenylmethylsulfonyl fluoride) and incubated on ice for 1 h. The solution was centrifuged at 15,000 × *g* for 30 min, and the supernatants were used as cell lysates. Fifty micrograms of protein from each sample were added to 3× SDS sample buffer (New England Biolabs Inc.) and boiled at 100 °C for 5 min. The samples were fractionated on a 2–15% SDS-polyacrylamide gel gradient (Daiichi Pure Chemicals Co., Ltd.). Gels were stained with Coomassie brilliant blue and dried on Whatman 3MM paper (Whatman International Ltd.). The radiolabeled materials were detected by using a BAS-2000 imaging analyzer (Fuji Photo Film).

Flow Cytometric Analysis—The HCT116 cells were subcultured onto 10-cm dishes at a concentration of 1.5 or 2 × 10⁶ cells/dish 72 h after transfection and 24 h prior to the analysis. These cells were then harvested with PBS containing 1 mM EDTA and washed with a wash buffer (PBS containing 0.1% bovine serum albumin and 0.1% sodium azide). Cell suspensions of 100 μ l (0.5 × 10⁶ cells) were incubated with G72 mAb (27) for 1 h on ice and washed twice with 0.5 ml of the wash buffer. The cells were then resuspended in 100 μ l of FITC-conjugated goat anti-mouse IgM and incubated on ice for 30 min. The cells were washed twice with wash buffer and resuspended in 500 μ l of PBS containing 0.1% sodium azide. Flow cytometric analysis was performed using FACSAria flow cytometer (BD Biosciences) and WinMDI 2.8 software (The Scripps Research Institute Cytometry software page).

RESULTS

Molecular Cloning of Human PAPST2 cDNA—We identified a cDNA sequence (GenBankTM Accession number NM_015948) homologous to the putative nucleotide sugar transporter gene *UGTrel1* by using the same procedure that was employed for the *PAPST1* gene (3). Initially, it was described as CGI-19 protein in the GenBankTM data base. We named it *PAPST2* and cloned the open reading frame as described under "Experimental Procedures." The phylogenetic tree of PAPS and the nucleotide sugar transporter genes in humans and *Drosophila* indicated that *PAPST1*, *PAPST2*, and *UGTrel1* are classified in the same group (Fig. 1A). An alignment of the amino acid sequences of these genes is shown in Fig. 1B. *PAPST2* comprised 401 amino acids with a calculated mass of 44.6 kDa. Hydrophobicity analyses of the amino acid sequences indicate that the *PAPST2* protein is a type III transmembrane protein with nine transmembrane domains similar to that of *PAPST1*, although the transmembrane topology has yet to be verified experimentally.

PAPST2 showed 22.4 and 21.7% identity to *UGTrel1* and *PAPST1*, respectively. The structural similarity suggested that *PAPST2* is a PAPS transporter gene similar to *PAPST1*. There are eight potential *N*-glyco-

sylation sites in the PAPST2. The *PAPST2* gene is mapped on human chromosome 6p24.3, and the mRNA comprises 11 exons.

PAPST2 Is a Golgi-localized Protein—PAPST1 is a membrane protein that is localized on the Golgi apparatus (3). Because PAPST2 shares similarity to PAPST1, we expected that PAPST2 would also be a Golgi-localized PAPS transporter.

First, we investigated the subcellular localization of the PAPST2 protein. Human colon cancer HCT116 cells were transiently transfected with a mammalian expression vector, pCXN2, that contained HA-tagged *PAPST2* or HA-tagged *PAPST1* gene and were double

immunostained with anti-HA mAb and anti- β 1,4 galactosyltransferase 1 mAb. The results of immunofluorescence microscopy of the cells are shown in Fig. 2A. The HA-tagged PAPST1 protein was observed to be colocalized with β 1,4 galactosyltransferase 1, which is a protein that is typically localized in the trans-Golgi (21), and this observation is consistent with a previous report (3). In this study, HA-tagged PAPST2 was also observed to be colocalized with β 1,4 galactosyltransferase 1, thereby indicating trans-Golgi localization.

To confirm whether PAPST1 and PAPST2 proteins possess identical subcellular localization, an experiment was performed wherein HA-tagged *PAPST2* and c-Myc-tagged *PAPST1* were expressed simultaneously in HCT116 cells. The cells were double immunostained with rhodamine-conjugated anti-HA mAb and FITC-conjugated anti-c-Myc mAb. As shown in Fig. 2B, PAPST2-HA was completely colocalized with PAPST1-c-Myc. These results indicate that the PAPST2 protein localizes on the Golgi apparatus like the PAPST1 protein.

Tissue Distribution of PAPST1 and PAPST2 Transcripts—Next, we analyzed the tissue distribution of *PAPST2* transcripts using real-time PCR. All transcript levels are shown relative to that of *GAPDH*. As shown in Fig. 3A, *PAPST2* is highly expressed in the colon, whereas the expression level of *PAPST1* is low. *PAPST2* transcripts are also widely expressed in other tissues when compared with that of *PAPST1* (Fig. 3A). To confirm the expression of *PAPST2* transcripts in the colon, we performed Northern blot analysis of RNAs that were derived from colon cancer cell lines HCT116 and DLD-1 and normal human colon tissue. The *PAPST2* mRNA was detected as a single band corresponding to 2 kbp (Fig. 3B), which is consistent with the length of the identified sequence, namely, NM_015948 (2068 bp). We expected that *PAPST2* would be a PAPS transporter gene that functions by compensating for the insufficient expression of *PAPST1* during the synthesis of sulfated glycoconjugates in the colon.

PAPST2 Is a PAPS Transporter Gene—The substrate specificity of the PAPST2 protein was examined by yeast expression in a manner similar to that used for PAPST1 (3). The yeast expression vector YE352GAP-II was inserted with HA-tagged *PAPST2* and introduced into W303-1a yeast for the preparation of the Golgi-enriched P100 membrane fraction that expressed the PAPST2 protein. The HA-tagged PAPST2 protein was detected in the yeast P100 membrane fraction by Western blotting using an antibody against the HA epitope tag (Fig. 4A).

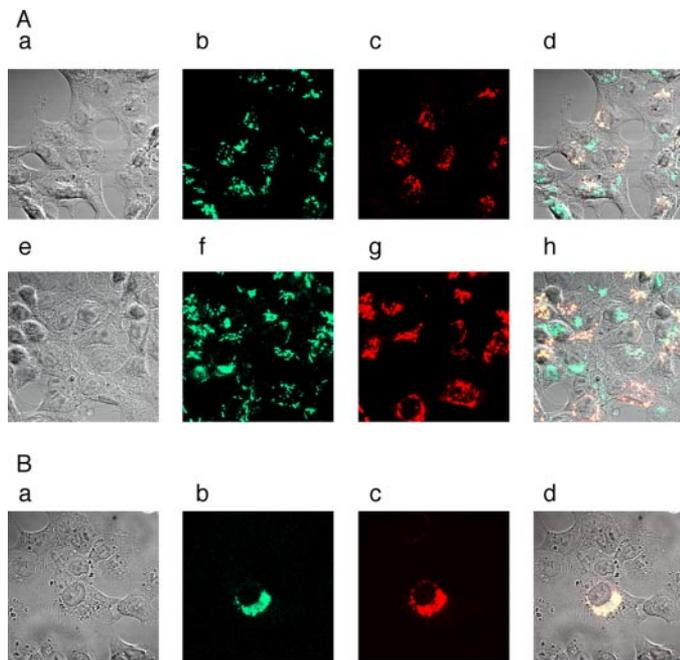


FIGURE 2. Both *PAPST1* and *PAPST2* are Golgi-localized proteins. A, HCT116 cells were transfected with HA-tagged *PAPST2* (a–d) or HA-tagged *PAPST1* (e–h) and analyzed using indirect immunofluorescence. Double staining was performed for the HA tag (b and f) and β 1,4 galactosyltransferase 1 (c and g). The images of HA and β 1,4 galactosyltransferase 1 were merged (d and h). B, HCT116 cells were simultaneously transfected with c-Myc-tagged *PAPST1* and HA-tagged *PAPST2*. Double staining was performed for the c-Myc tag (b) and HA tag (c). The images of HA and β 1,4 galactosyltransferase 1 were merged (d). The scale at the bottom represents 20 μ m.

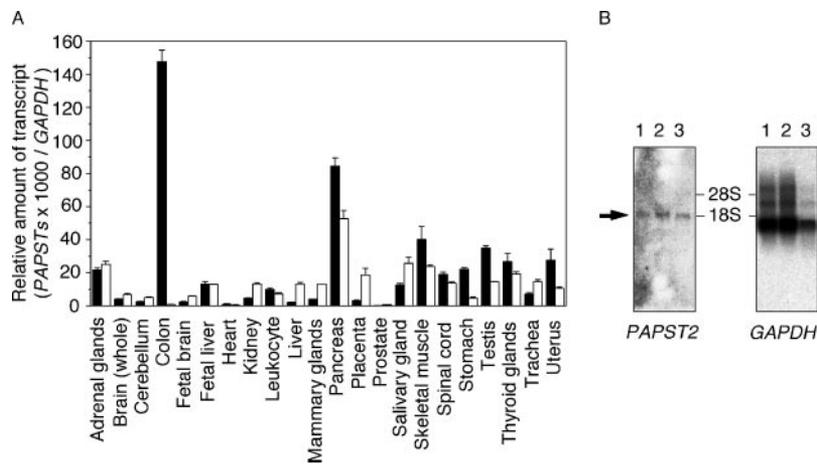


FIGURE 3. Tissue distribution of the *PAPST1* and *PAPST2* transcripts. A, quantitative analysis of the *PAPST1* and *PAPST2* transcripts in human tissues by real-time PCR. The expression levels of the *PAPST1* and *PAPST2* transcripts were normalized with respect to those of the *GAPDH* transcript, which was measured in the same cDNAs. The indicated values are the mean \pm S.E. obtained from four measurements. Open bars, *PAPST1*; Solid bars, *PAPST2*. B, Northern blot analysis of *PAPST2* in the human colon. The poly(A)⁺ RNAs prepared from two human colon cancer cell lines, namely, HCT116 and DLD-1, and normal human colon tissue were blotted on a nylon membrane and hybridized with the probe for *PAPST2* (left panel) as described under “Experimental Procedures.” The right panel shows the signal detected by the probe for *GAPDH* on the same membrane. The positions of 18 and 28 S ribosomal RNA are indicated. Lanes 1, HCT116; lanes 2, DLD-1; lanes 3, normal colon. Arrow indicates the approximate location of the *PAPST2*.

PAPST2, a Novel Human PAPS Transporter

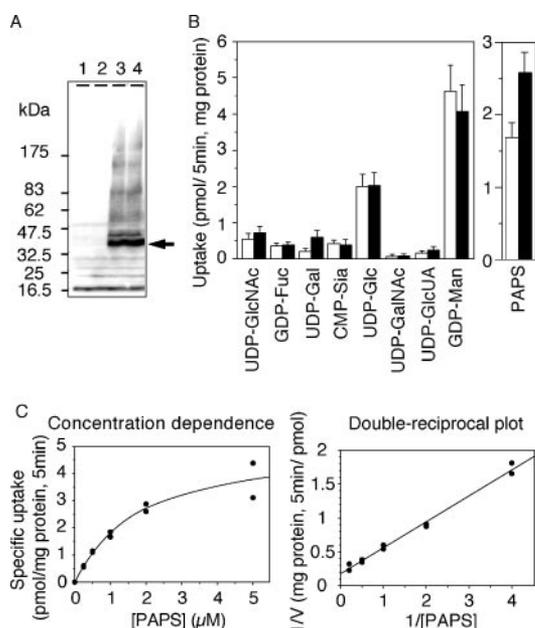


FIGURE 4. PAPST2 is a PAPS transporter. *A*, expression state of PAPST2 protein in the Golgi-enriched fraction. Each P100 fraction (50 μ g of protein), prepared from yeast cells expressing either the mock vector (lanes 1 and 2) or HA-tagged PAPST2 (lanes 3 and 4), was subjected to SDS-polyacrylamide electrophoresis. Western blot analysis was performed using a monoclonal antibody against the HA epitope. Arrow indicates HA-tagged PAPST2. *B*, substrate specificity of PAPST2. Each P100 fraction (200 μ g of protein) was incubated in 100 μ l of reaction buffer containing 1 μ M substrate at 30 °C for 5 min, and the incorporated radioactivity was measured. The indicated values are the mean \pm S.E. obtained from six independent experiments. Each experiment was performed with two transformant clones. Open bars, Mock; solid bars, PAPST2. *C*, substrate concentration dependence. Each P100 fraction (200 μ g of protein) was incubated in 100 μ l of reaction buffer containing different concentrations of [³⁵S]PAPS at 30 °C for 5 min, and the incorporated radioactivity was measured. Specific incorporation was calculated by subtracting the value of the mock transfection from each of the corresponding values. Right panel shows the double-reciprocal plot used to determine the K_m value.

The substrate specificity of the PAPST2 protein was examined using the P100 membrane fraction and radiolabeled substrates. The transport activity of PAPS into the P100 membrane fraction is shown in Fig. 4*B*. The P100 membrane fraction prepared from yeast cells that expressed PAPST2 showed PAPS transport activity that was significantly higher than that observed in the mock cells (1.7 ± 0.2 versus 2.6 ± 0.3 pmol/mg of protein, respectively, mean \pm S.E. from six independent experiments; $p < 0.05$, Student's *t*-test), although the yeast Golgi-enriched fraction had relatively high endogenous PAPS transport activity. The substrate concentration dependence of PAPS transport by PAPST2 is shown in Fig. 4*C*. PAPST2 showed a saturated PAPS transport activity with an apparent K_m value that was estimated to be 2.2 μ M.

Both PAPST1 and PAPST2 Transport PAPS in the Human Colon Cancer Cell Line—We also tested the PAPS transport activity of PAPST2 protein by using a mammalian cell line. For measuring the PAPS transport activity, we analyzed the Golgi-enriched fractions of colon cancer HCT116 cells that stably expressed HA-tagged PAPST1, HA-tagged PAPST2, or the mock vector (pCXN2 vector alone).

As shown in Fig. 5*A*, the levels of PAPST1 and PAPST2 transcripts in the PAPST1 and PAPST2 transfectant cells, respectively, showed a marked increase over those obtained from the mock transfectants. No difference was observed between the mock and PAPST1 transfectants with respect to PAPST2 transcript levels or between the mock and PAPST2 transfectants with respect to PAPST1 transcript levels (Fig. 5*A*). In each transfectant, HA-tagged PAPST1 or HA-tagged PAPST2 protein was detected in the Golgi-enriched fraction by Western blotting using an antibody against the HA epitope tag (Fig. 5*B*). The PAPS transport activity that was obtained from each Golgi-enriched fraction is

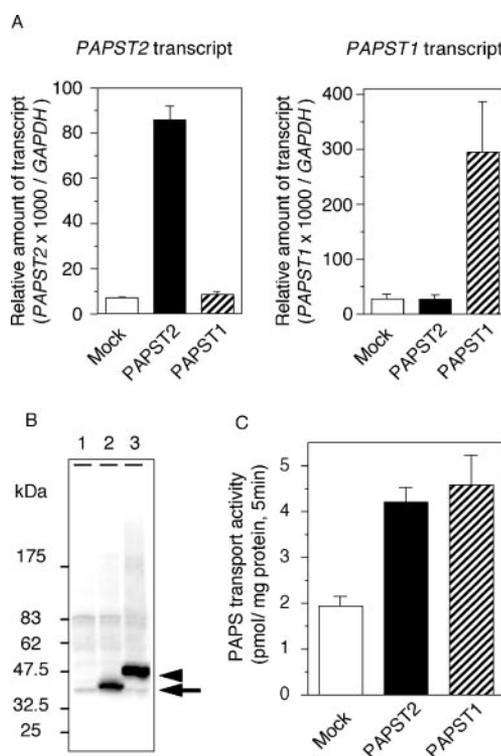


FIGURE 5. Both PAPST1 and PAPST2 transport PAPS in human colon cancer cell line. *A*, expression levels of PAPST1 and PAPST2 transcripts in each transfectant. The relative amounts of each transcript were normalized with respect to those of the GAPDH transcript, which was measured in the same cDNAs. The indicated values are the mean \pm S.E. obtained from three independent measurements. *B*, expression states of the PAPST1 and PAPST2 proteins in each transfectant. Each Golgi-enriched fraction (10 μ g of protein) prepared from the HCT116 cells that stably expressed mock vector (lane 1), HA-tagged PAPST2 (lane 2), or HA-tagged PAPST1 (lane 3) was subjected to SDS-polyacrylamide electrophoresis. Western blot analysis was performed using a monoclonal antibody against a HA epitope. Arrow and arrowhead indicate HA-tagged PAPST2 and HA-tagged PAPST1, respectively. *C*, PAPS transport activity. Each Golgi-enriched fraction (100 μ g of protein) was incubated in 100 μ l of the reaction buffer containing 1 μ M [³⁵S]PAPS at 30 °C for 5 min, and the incorporated radioactivity was measured. Values shown are the mean \pm S.E. obtained from three independent experiments.

shown in Fig. 5*C*. These Golgi-enriched fractions also showed relatively high endogenous PAPS transport activity; however, the value observed in the PAPST2 transfectants was significantly higher than that observed in the mock transfectants (1.9 ± 0.2 versus 4.2 ± 0.3 pmol/mg of protein, respectively, mean \pm S.E. from three independent experiments; $p < 0.05$, Student's *t*-test). These results indicate that both PAPST1 and PAPST2 act as PAPS transporters in the human colon cancer cell line.

PAPST2 Is Involved in the Synthesis of Sulfated Glycoconjugates in the Human Colon—We revealed that PAPST2 is a PAPS transporter that is expressed in the colon. To elucidate the role of PAPST2 in the synthesis of sulfated glycoconjugates in the colon, we performed a flow cytometric analysis of the colon cancer cell line by using an antibody, G72, recognizing sialyl 6-sulfo *N*-acetylglucosamine (sialyl 6-sulfo galactose β 1,4 *N*-acetyl D-glucosamine: Sia α 2,3 Gal β 1,4 GlcNAc that is sulfated at the C-6 position of GlcNAc) (27). We attempted to reduce PAPST2 expression in the colon cancer cell line HCT116, which is moderately reactive to G72 antibody, by using RNAi. Based on their ability to suppress gene expression, two siRNA sequences that would target the PAPST1 and PAPST2 genes, *i.e.* PAPST1-813 and PAPST2-513, respectively, were selected. These siRNAs were synthesized as double-stranded stealth RNAs (Invitrogen) possessing 25 nucleotides, and the stealth RNAi negative control duplex (Invitrogen) was used as a control siRNA. Lipofection was used to transfect the HCT116 cells with 10 nM PAPST1-813 and PAPST2-513 siRNAs.

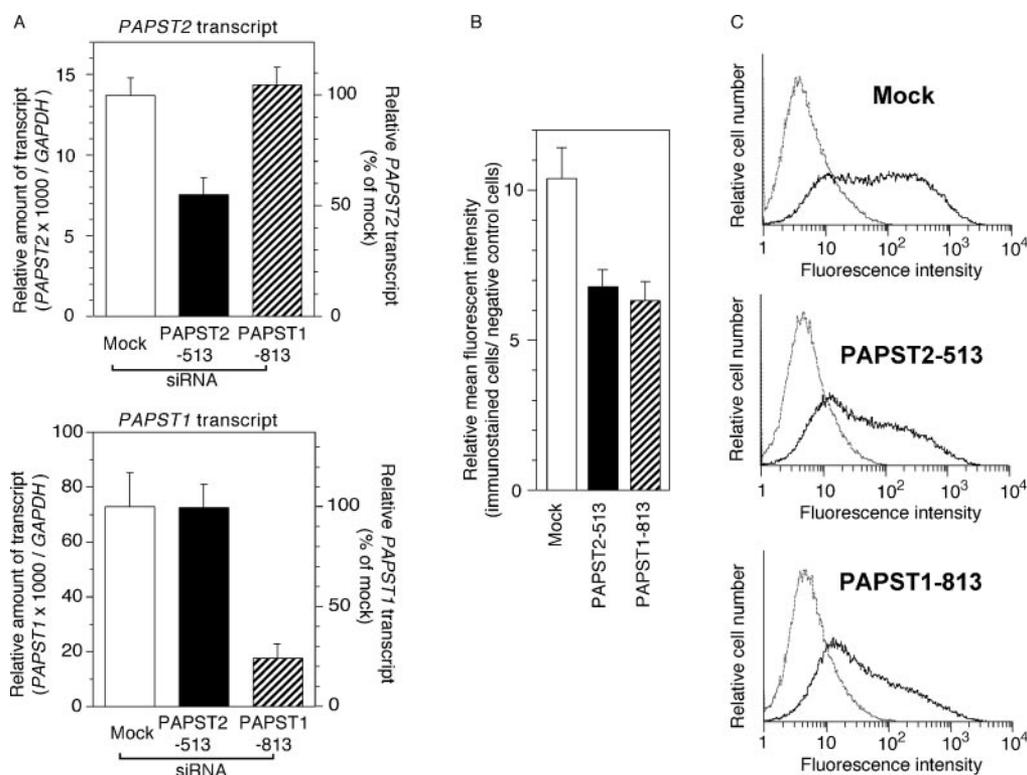


FIGURE 6. **Flow cytometric analysis of HCT116 cells transfected with siRNAs.** HCT116 cells were transfected with mock siRNA, *PAPST2* siRNA (*PAPST2*-513), or *PAPST1* siRNA (*PAPST1*-813) at a concentration of 10 nM by using Lipofectamine 2000 reagent. The cells were harvested and analyzed 96 h after transfection. **A**, knockdown efficiency of each siRNA for the *PAPST1* and *PAPST2* transcripts. Relative amounts of each transcript were quantified by real-time PCR. The indicated values are the mean ± S.E. obtained from three independent experiments. **B**, relative mean fluorescent intensity. Cells treated with each siRNA were immunostained with G72 mAb and analyzed by flow cytometry. The values of mean fluorescent intensity were adjusted with respect to those of the negative control cells. The indicated values are the mean ± S.E. obtained from three independent experiments. **C**, a representative result of flow cytometric analysis. *Faint, dotted lines* indicate the negative controls stained with FITC-conjugated anti-mouse IgM without the primary antibody.

The cells were harvested and immunostained with G72 antibody 96 h after transfection. The efficiency of gene silencing was determined by real-time PCR. As shown in Fig. 6A, transfection using the *PAPST2*-513 and *PAPST1*-813 siRNAs resulted in a 45 and 76% knockdown of the corresponding mRNAs, respectively. Results of the flow cytometric analysis of the cells treated with siRNAs are shown in Fig. 6B. The cells treated with *PAPST2*-513 siRNA showed significantly reduced G72 reactivity when compared with that of control siRNA (averaged relative mean fluorescence intensity for mock, 10.4 ± 1.0 and for *PAPST2*, 6.8 ± 0.5; mean ± S.E. from three independent experiments, *p* < 0.05, Student's *t*-test). On the other hand, transfection of *PAPST1*-813 siRNA showed similar moderate decrease in G72 reactivity despite the greater reduction of the *PAPST1* gene. This indicates that *PAPST2* plays a role in the synthesis of the sialyl 6-sulfo galactose β1,4 *N*-acetyl D-glucosamine epitope in this cell line. We obtained similar results when another siRNA sequence targeted the *PAPST2* gene (*PAPST2*-342) at a concentration of 100 nM (averaged mean fluorescence intensity for mock, 4.0 ± 1.0; for *PAPST2*-513, 2.4 ± 0.2; for *PAPST2*-342, 2.1 ± 0.4; and for *PAPST1*-813, 2.8 ± 0.3, mean ± S.E. from four independent experiments).

We also determined total sulfate incorporation into cellular proteins in the HCT116 cells by metabolic labeling with [³⁵S]sulfate. As shown in Fig. 7A, transfection of both *PAPST2*-513 and *PAPST1*-813 siRNAs reduced the [³⁵S]sulfate-labeled proteins. The density of radioactivity in each lane of the SDS-PAGE is shown in Fig. 7C. The *PAPST1*-813- and *PAPST2*-513-transfected cells resulted in a radioactivity density of 83.0% ± 2.3 and 90.2% ± 3.7 as compared with that of mock siRNA, respectively (mean ± S.E. from three independent experiments; *p* < 0.05 for *PAPST2*-513 *versus* mock, Student's *t*-test). Transfection using the *PAPST2*-513 and *PAPST1*-813 siRNAs resulted in a 30 and 69% knockdown of the corre-

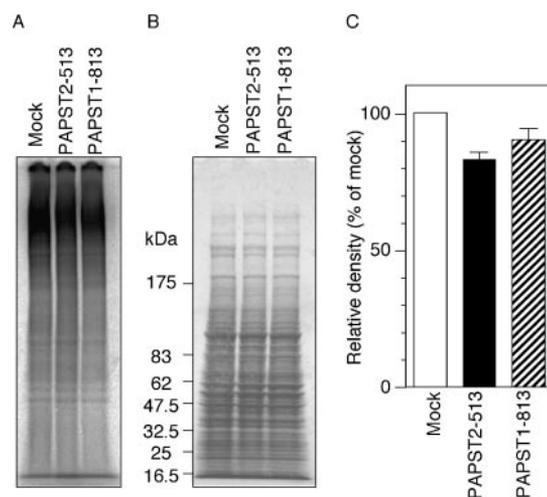


FIGURE 7. **Metabolic labeling of HCT116 cells transfected with siRNAs.** **A**, HCT116 cells were transfected with mock siRNA, *PAPST2* siRNA (*PAPST2*-513), or *PAPST1* siRNA (*PAPST1*-813) at a concentration of 10 nM by using Lipofectamine 2000 reagent. Forty-eight hours after transfection, cells were metabolically labeled with [³⁵S]sulfate and cultured for 48 h. The cell lysate of each transfectant (50 μg of protein) was subjected to SDS-polyacrylamide electrophoresis. The radioactive compounds were detected as described under "Experimental Procedures." **B**, the Coomassie brilliant blue-stained image of the same gel. **C**, the density of radioactive bands in each lane was calculated using the public domain NIH image program (developed by the U. S. National Institutes of Health) and normalized with respect to those of the Coomassie brilliant blue-stained image. Values shown are the mean ± S.E. obtained from three independent experiments. Values obtained for the mock siRNA are presented as 100%.

sponding mRNAs, respectively. These results demonstrated that *PAPST2* is a PAPS transporter gene that is involved in the synthesis of sulfated glycoconjugates in the colon.

DISCUSSION

We identified a novel human PAPS transporter that is predominantly expressed in the colon. Human colonic epithelial tissues express many sulfated glycoconjugates. Silencing of the *PAPST2* gene by RNAi caused a reduction in the amount of sulfated structures in the colon cancer cell line. Expression of small amounts of *PAPST1* mRNA in the colon suggests that *PAPST2* plays a major role in the sulfation of glycoconjugates in this organ.

The *PAPST2* gene is closely related to the *PAPST1* gene, and the genomic locus of the *PAPST2* gene is located close to that of *PAPST1* (6p24.3 and 6p11.2–12.1, respectively). Despite their functional conservation, the genomic structures of *PAPST2* and *PAPST1* are not similar (eleven exons versus four exons, respectively). Furthermore, both *PAPST1* and *PAPST2* have a single ortholog in *Drosophila*, namely, *sll* and NM_140697, respectively (Fig. 1A).³ These findings indicate that during the evolutionary process, the *PAPST1* and *PAPST2* genes diverged relatively early and thereafter evolved independently.

Recently, the nucleotide sugar transporter genes have been classified into the solute carrier family 35 (SLC35) (28). The *PAPST1* and *PAPST2* genes have also been classified into the SLC35 subfamily B. In GenBankTM, *UGTrel1*, *PAPST1*, and *PAPST2* have been defined as members of B1 (*SLC35B1*), B2 (*SLC35B2*), and B3 (*SLC35B3*), respectively. More recently, Ashikov *et al.* (29) reported that another member of subfamily B, namely, *SLC35B4*, is a UDP-xylose/UDP-GlcNAc transporter gene. Data bases mention that *SLC35B4* is a human ortholog of yeast UDP-GlcNAc transporter genes, namely, *Kluyveromyces lactis mnn2-2* (30) and *S. cerevisiae yea4* (31). This implies that the subfamily B comprises members with entirely different substrate specificities despite their structural conservation.

Silencing of *PAPST2* gene expression in the colon cancer cell line revealed the involvement of PAPST2 in the synthesis of a sulfated epitope, sialyl 6-sulfo galactose β 1,4 *N*-acetyl D-glucosamine (Fig. 6). The fucosylated derivative, namely, sialyl 6-sulfo Le^x, is a major L-selectin ligand present on the high endothelial venules of the human peripheral lymph nodes for the initial adhesion of leukocytes to endothelial cells (27, 32–34). It has been proposed that sialyl 6-sulfo Le^x serves as a ligand for selectins in routine trafficking of leukocytes, whereas non-sulfated sialyl Le^x plays a major role in the inflammatory response (35, 36). PAPST2 may be involved in the function of these physiological routine processes, including the recruitment of gut-homing helper memory T lymphocytes, by regulating the sulfation of carbohydrate epitopes.

It is common knowledge that the risk of malignancy and recurrence of colorectal cancer is correlated with an increase in sialylation (13, 15, 16) and a decrease in the sulfation of carbohydrate epitopes (11–14). The sialyl 6-sulfo Le^x (14) and 3'-sulfo-Le^a (13, 17) are predominantly expressed in nonmalignant tissues but are not detected in the malignant tissues in colorectal cancers. Kumamoto *et al.* (37) reported that in colorectal cancers the expression of the UDP-Gal transporter increases significantly and results in the supply of the donor substrate for the synthesis of sialyl Le^a and sialyl Le^x. On the other hand, the colon cancer cell line HCT116 showed relatively low *PAPST2* expression when compared with that of normal colon tissue. We could not find any colon cancer cell line that highly expressed *PAPST2*. The possibility that *PAPST2* decreases the expression associated with the progression of colorectal cancer, as reported in the case of certain sulfotransferases (38–40) and a sulfate transporter (41), may be considered.

The RNAi of *PAPST2* gene in the HCT116 cells reduced total sulfate

incorporation into cellular proteins. The sulfotransferases have long been believed to be the rate-limiting components of the sulfation process; however, sulfation is also controlled by the components involved in the earlier steps, such as the sulfate transporters and PAPS synthetases (42). For instance, PAPS synthetases modulate PAPS levels in high endothelial venules and thus play a key role in the control of the sulfation state of L-selectin ligands and its functional activities (43–45). Furthermore, mutations in some genes involved in PAPS synthesis, such as diastrophic dysplasia sulfate transporter (*DTDST*) (46–49) and PAPS synthetase 2 (*PAPSS2*) (2, 50), are responsible for a form of human-inherited osteochondrodysplasias that results because of down-regulated sulfation of chondroitin sulfate in the cartilage. This evidence implies that PAPS production is a rate-limiting step for sulfation in certain tissues. Our investigation also demonstrated that the PAPS transporter is a rate-limiting factor in the sulfation of glycoconjugates in the colon cells. The PAPST2 protein showed a relatively low apparent K_m value for PAPS (2.2 μ M), although the precise kinetics of PAPST2 protein, excluding other factors, remains uncertain. The effect of the PAPS transporter would be significant if the K_m value for PAPS would be lower than the K_m value of the sulfotransferases in the Golgi lumen.

In the previous study, we reported that *sll*, the *PAPST1* ortholog in *Drosophila*, is essential for viability of the fly (3). Lüders *et al.* (4) demonstrated that *sll* gene is involved in the signaling pathways and that the mutation of *sll* gene exhibits disrupted Wingless gradient and reduced Hedgehog signaling activity. Here, both PAPST1 and PAPST2 are shown to be Golgi-localized PAPS transporters. Most sulfation reactions of glycoconjugates, including proteoglycans (51), glycoproteins (52), and glycolipids (53), occur in the Golgi apparatus. Furthermore, tyrosine *O*-sulfation of the proteins occurs in the trans-Golgi network (54, 55). In most human tissues, the expression of *PAPST2* is comparable with that of *PAPST1* (Fig. 3). The PAPST1 and PAPST2 proteins have comparable K_m values for PAPS (0.8 versus 2.2 μ M, respectively). PAPST1 and PAPST2 may function in a manner that is complementary to each other. Further investigations are required to clarify the involvement and significance of PAPST1 and PAPST2 in these pathways.

REFERENCES

- Li, H., Deyrup, A., Mensch, J. R., Jr., Domowicz, M., Konstantinidis, A. K., and Schwartz, N. B. (1995) *J. Biol. Chem.* **270**, 29453–29459
- Kurima, K., Warman, M. L., Krishnan, S., Domowicz, M., Krueger, R. C., Jr., Deyrup, A., and Schwartz, N. B. (1998) *Proc. Natl. Acad. Sci. U. S. A.* **95**, 8681–8685
- Kamiyama, S., Suda, T., Ueda, R., Suzuki, M., Okubo, R., Kikuchi, N., Chiba, Y., Goto, S., Toyoda, H., Saigo, K., Watanabe, M., Narimatsu, H., Jigami, Y., and Nishihara, S. (2003) *J. Biol. Chem.* **278**, 25958–25963
- Lüders, F., Segawa, H., Stein, D., Selva, E. M., Perrimon, N., Turco, S. J., and Häcker, U. (2003) *EMBO J.* **22**, 3635–3644
- Reichsman, F., Smith, L., and Cumberledge, S. (1996) *J. Cell Biol.* **135**, 819–827
- Zioncheck, T. F., Richardson, L., Liu, J., Chang, L., King, K. L., Bennett, G. L., Fugedi, P., Chamow, S. M., Schwall, R. H., and Stack, R. J. (1995) *J. Biol. Chem.* **270**, 16871–16878
- Olwin, B. B., and Rapraeger, A. (1992) *J. Cell Biol.* **118**, 631–639
- Yayon, A., Klagsbrun, M., Esko, J. D., Leder, P., and Ornitz, D. M. (1991) *Cell* **64**, 841–848
- Rapraeger, A. C., Krufka, A., and Olwin, B. B. (1991) *Science* **252**, 1705–1708
- Aviezer, D., and Yayon, A. (1994) *Proc. Natl. Acad. Sci. U. S. A.* **91**, 12173–12177
- Irimura, T., Wynn, D. M., Hager, L. G., Cleary, K. R., and Ota, D. M. (1991) *Cancer Res.* **51**, 5728–5735
- Yamori, T., Ota, D. M., Cleary, K. R., Hoff, S., Hager, L. G., and Irimura, T. (1989) *Cancer Res.* **49**, 887–894
- Matsushita, Y., Yamamoto, N., Shirahama, H., Tanaka, S., Yonezawa, S., Yamori, T., Irimura, T., and Sato, E. (1995) *Jpn. J. Cancer Res.* **86**, 1060–1067
- Izawa, M., Kumamoto, K., Mitsuoka, C., Kanamori, C., Kanamori, A., Ohmori, K., Ishida, H., Nakamura, S., Kurata-Miura, K., Sasaki, K., Nishi, T., and Kannagi, R. (2000) *Cancer Res.* **60**, 1410–1416
- Nakayama, T., Watanabe, M., Katsumata, T., Teramoto, T., and Kitajima, M. (1995) *Cancer Res.* **75**, 2051–2056
- Nakamori, S., Kameyama, M., Imaoka, S., Furukawa, H., Ishikawa, O., Sasaki, Y.,

³ E. Goda and S. Nishihara, unpublished observation.

- Kabuto, T., Iwanaga, T., Matsushita, Y., and Irimura, T. (1993) *Cancer Res.* **53**, 3632–3637
17. Yamachika, T., Nakanishi, H., Inada, K., Kitoh, K., Kato, T., Irimura, T., and Tatematsu, M. (1997) *Virchows Arch.* **431**, 25–30
 18. Ishida, N., Miura, N., Yoshioka, S., and Kawakita, M. (1996) *J. Biochem.* **120**, 1074–1078
 19. Suda, T., Kamiyama, S., Suzuki, M., Kikuchi, N., Nakayama, K., Narimatsu, H., Jigami, Y., Aoki, T., and Nishihara, S. (2004) *J. Biol. Chem.* **279**, 26469–26474
 20. Niwa, H., Yamamura, K., and Miyazaki, J. (1991) *Gene* **108**, 193–199
 21. Uemura, M., Sakaguchi, T., Uejima, T., Nozawa, S., and Narimatsu, H. (1992) *Cancer Res.* **52**, 6153–6157
 22. Ito, H., Fukuda, Y., Murata, K., and Kimura, A. (1983) *J. Bacteriol.* **153**, 163–168
 23. Nakayama, K., Maeda, Y., and Jigami, Y. (2003) *Glycobiology* **13**, 673–680
 24. Chomczynski, P., and Sacchi, N. (1987) *Anal. Biochem.* **162**, 156–159
 25. Ui-Tei, K., Naito, Y., Takahashi, F., Haraguchi, T., Ohki-Hamazaki, H., Juni, A., Ueda, R., and Saigo, K. (2004) *Nucleic Acids Res.* **32**, 936–948
 26. Tsuiji, H., Hayashi, M., Wynn D. M., and Irimura, T. (1998) *Jpn. J. Cancer Res.* **89**, 1267–1275
 27. Mitsuoka, C., Sawada-Kasugai, M., Ando-Furui, K., Izawa, M., Nakanishi, H., Nakamura, S., Ishida, H., Kiso, M., and Kannagi, R. (1998) *J. Biol. Chem.* **273**, 11225–11233
 28. Ishida, N., and Kawakita, M. (2004) *Pflugers Arch.* **447**, 768–775
 29. Ashikov, A., Routier, F., Fuhlrott, J., Helmus, Y., Wild, M. K., Gerardy-Schahn, R., and Bakker, H. (2005) *J. Biol. Chem.* **280**, 27230–27235
 30. Abeijon, C., Robbins, P. W., and Hirschberg, C. B. (1996) *Proc. Natl. Acad. Sci. U. S. A.* **93**, 5963–5968
 31. Roy, S. K., Chiba, Y., Takeuchi, M., and Jigami, Y. (2000) *J. Biol. Chem.* **275**, 13580–13587
 32. Mitsuoka, C., Kawakami-Kimura, N., Kasugai-Sawada, M., Hiraiwa, N., Toda, K., Ishida, H., Kiso, M., Hasegawa, A., and Kannagi, R. (1997) *Biochem. Biophys. Res. Commun.* **230**, 546–551
 33. Hemmerich, S., Bertozzi, C. R., Leffler, H., and Rosen, S. D. (1994) *Biochemistry* **33**, 4820–4829
 34. Kimura, N., Mitsuoka, C., Kanamori, A., Hiraiwa, N., Uchimura, K., Muramatsu, T., Tamatani, T., Kansas, G. S., and Kannagi, R. (1999) *Proc. Natl. Acad. Sci. U. S. A.* **96**, 4530–4535
 35. Kannagi, R., and Kanamori, A. (1999) *Trends Glycosci. Glycotech.* **11**, 329–344
 36. Kannagi, R. (2002) *Curr. Opin. Struct. Biol.* **12**, 599–608
 37. Kumamoto, K., Goto, Y., Sekikawa, K., Takenoshita, S., Ishida, N., Kawakita, M., and Kannagi, R. (2001) *Cancer Res.* **61**, 4620–4627
 38. Seko, A., Sumiya, J., Yonezawa, S., Nagata, K., and Yamashita, K. (2000) *Glycobiology* **10**, 919–929
 39. Uchimura, K., El-Fasakhany, F. M., Hori, M., Hemmerich, S., Blink, S. E., Kansas, G. S., Kanamori, A., Kumamoto, K., Kannagi, R., and Muramatsu, T. (2002) *J. Biol. Chem.* **277**, 3979–3984
 40. Seko, A., Nagata, K., Yonezawa, S., and Yamashita, K. (2002) *Jpn. J. Cancer Res.* **93**, 507–515
 41. Antalis, T. M., Reeder, J. A., Gotley, D. C., Byeon, M. K., Walsh, M. D., Henderson, K. W., Papas, T. S., and Schweinfest, C. W. (1998) *Clin. Cancer Res.* **4**, 1857–1863
 42. Kamiyama, S., and Nishihara, S. (2004) *Trends Glycosci. Glycotech.* **16**, 109–123
 43. Hemmerich, S., Butcher, E. C., and Rosen, S. D. (1994) *J. Exp. Med.* **180**, 2219–2226
 44. Girard, J. P., Baekkevold, E. S., and Amalric, F. (1998) *FASEB J.* **12**, 603–612
 45. Imai, Y., Lasky, L. A., and Rosen, S. D. (1993) *Nature* **361**, 555–557
 46. Superti-Furga, A., Neumann, L., Riebel, T., Eich, G., Steinmann, B., Spranger, J., and Kunze, J. (1999) *J. Med. Genet.* **36**, 621–624
 47. Superti-Furga, A., Hästbacka, J., Wilcox, W. R., Cohn, D. H., van der Harten, H. J., Rossi, A., Blau, N., Rimoin, D. L., Steinmann, B., Lander, E. S., and Gitzelmann, R. (1996) *Nat. Genet.* **12**, 100–102
 48. Hästbacka, J., Superti-Furga, A., Wilcox, W. R., Rimoin, D. L., Cohn, D. H., and Lander, E. S. (1996) *Am. J. Hum. Genet.* **58**, 255–262
 49. Hästbacka, J., de la Chapelle, A., Mahtani, M. M., Clines, G., Reeve-Daly, M. P., Daly, M., Hamilton, B. A., Kusumi, K., Trivedi, B., Weaver, A., Coloma, A., Lovet, M., Buckler, A., Kaitila, I., and Lander, E. S. (1994) *Cell* **78**, 1073–1087
 50. ul Haque, M. F., King, L. M., Krakow, D., Cantor, R. M., Rusiniak, M. E., Swank, R. T., Superti-Furga, A., Haque, S., Abbas, H., Ahmad, W., Ahmad, M., and Cohn, D. H. (1998) *Nat. Genet.* **20**, 157–162
 51. Salmivirta, M., Lidholt, K., and Lindahl, U. (1996) *FASEB J.* **10**, 1270–1279
 52. Lane, N., Caro, L., Otero Vilardebo, L. R., and Godman, G. C. (1964) *J. Cell Biol.* **21**, 339–351
 53. Fleischer, B., and Zambrano, F. (1974) *J. Biol. Chem.* **249**, 5995–6003
 54. Moore, K. L. (2003) *J. Biol. Chem.* **278**, 24243–24246
 55. Bauerle, P. A., and Huttner, W. B. (1987) *J. Cell Biol.* **105**, 2655–2664